DLK induces developmental neuronal degeneration via selective regulation of proapoptotic JNK activity

Arundhati Sengupta Ghosh, Bei Wang, Christine D. Pozniak, Mark Chen, Ryan J. Watts, and Joseph W. Lewcock

Neurodegeneration Laboratories, Department of Neuroscience, Genentech, Inc., South San Francisco, CA 94080

The c-Jun N-terminal kinase (JNK) signaling pathway is essential for neuronal degeneration in multiple contexts but also regulates neuronal homeostasis. It remains unclear how neurons are able to dissociate proapoptotic JNK signaling from physiological JNK activity. In this paper, we show that the mixed lineage kinase dual leucine zipper kinase (DLK) selectively regulates the JNK-based stress response pathway to mediate axon degeneration and neuronal apoptosis without influencing other aspects of JNK signaling. This specificity is dependent on interaction of DLK with the scaffolding protein JIP3 to form a specialized JNK signaling complex. Local activation of DLK-based signaling in the axon results in phosphorylation of c-Jun and apoptosis after redistribution of JNK to the cell body. In contrast, regulation of axon degeneration by DLK is c-Jun independent and mediated by distinct JNK substrates. DLK-null mice displayed reduced apoptosis in multiple neuronal populations during development, demonstrating that prodegenerative DLK signaling is required in vivo.

Introduction

The establishment of peripheral innervation during development requires axonal outgrowth to target regions and subsequent refinement of connectivity through the removal of exuberant neuronal processes and the elimination of excess neurons via apoptosis (Oppenheim, 1991; Luo and O'Leary, 2005). Developmental apoptosis has been extensively studied in sympathetic and dorsal root ganglion (DRG) neurons that depend on NGF for their survival (Levi-Montalcini and Booker, 1960; Crowley et al., 1994). In these neurons, loss of NGF signaling results in rapid degeneration (Gorin and Johnson, 1979). Regulators of the intrinsic apoptosis pathway including Bcl-2–associated X (BAX) protein and Bcl-2 have been implicated in this process (Garcia et al., 1992), and mice lacking a functional BAX gene lose significantly fewer neurons during development (Deckwerth et al., 1996; White et al., 1998). A c-Jun–dependent transcriptional program is also required for apoptosis to proceed, which is initiated after c-Jun phosphorylation by the JNK family of MAPKs (Ham et al., 1995; Whitfield et al., 2001; Palmada et al., 2002; Besirli et al., 2005). This parallels what has been observed after neuronal injury, in which phosphorylation of c-Jun and other downstream targets by JNK is necessary for neuronal cell death (Bogoyevitch, 2006).

The pathways that underlie the selective degeneration of neuronal processes in development and disease are less well defined, though a growing body of literature suggests that this degeneration is an active process that can be separated from neuronal apoptosis. This idea is supported by data demonstrating that expression of Wld^{s}, a gene fusion between UFD2/E4 and NMAT (nicotinamide nucleotide adenylyltransferase), is able to strongly protect axons but not cell bodies from degeneration (Mack et al., 2001). Recently, components of the intrinsic pathways that regulate axonal degeneration have also been identified. JNK signaling as well as the ubiquitin proteasome system and apoptotic caspases are essential for degeneration in certain experimental paradigms, though some model system–dependent differences have been observed (Watts et al., 2003; Miller et al., 2009; Nikolaev et al., 2009; Vohra et al., 2010).

The JNK pathway is required for both neuronal apoptosis and axon degeneration but also functions to regulate neuronal

Correspondence to Joseph W. Lewcock: lewcock.joseph@gene.com

Abbreviations used in this paper: BAX, Bcl-2–associated X; DLK, dual leucine zipper kinase; DRG, dorsal root ganglion; ERK, extracellular signal-regulated kinase; ES, embryonic stem; IP, immunoprecipitation; JIP, JNK-interacting protein; MLK, mixed lineage kinase; NeuN, neuronal nuclei; p-c-Jun, phosphorylated c-Jun; p-ERK; phosphorylated ERK; p-JNK, phosphorylated JNK; wt, wild type.

The Rockefeller University Press $30.00
J. Cell Biol. Vol. 194 No. 5 751–764
www.jcb.org/cgi/doi/10.1083/jcb.201103153

growth and homeostasis (Chang et al., 2003; Björkblom et al., 2005). Neurons contain high levels of activated JNK even in the absence of stress but have the ability to discriminate this basal activity from proapoptotic JNK signaling (Coffey et al., 2000). Studies using JNK-null mice have demonstrated that each of the three mammalian JNK genes has specific functions, which explains at least in part how this selectivity is achieved. For instance, mice lacking JNK2 and/or JNK3 are protected from stress-induced neuronal apoptosis and display reduced phosphorylation of stress-specific downstream targets such as c-Jun, whereas JNK1-null mice show no protection (Chang et al., 2003; Hunot et al., 2004; Yang et al., 1997). Additional selectivity is likely to be mediated via interaction of JNKs with JNK-interacting proteins (JIPs), which are thought to facilitate formation signaling complexes comprised of JNKs and upstream kinases (Whitmarsh, 2006). It has been hypothesized that specific combinations of JNK, JIP, and upstream kinases can lead to highly specific JNK signaling complexes with defined outputs (Waetzig and Herdegen, 2005), but few such complexes have been identified.

Experiments using the pan-mixed lineage kinase (MLK) inhibitor CEP-1347 have suggested that this family of kinases is a major upstream regulator of JNK activation in neurons (Maroney et al., 1998), yet the specific MLKs that control neuronal degeneration are not well defined. Recently, the MLK dual leucine zipper kinase (DLK) has been shown to play a role in neuronal injury–induced axonal degeneration, a function that is likely JNK mediated (Miller et al., 2009). In other contexts, however, DLK does not mediate degeneration and is instead required for axonal regeneration after injury (Hammarlund et al., 2009; Xiong et al., 2010). During development, DLK is a component of a pathway that regulates axon outgrowth and synapse formation via regulation of JNK and/or P38 MAPKs (Nakata et al., 2005; Collins et al., 2006; Hirai et al., 2006; Lewcock et al., 2007), and reduced DLK expression either directly or indirectly leads to increased numbers of spinal motor neurons (Itoh et al., 2011).

In this study, we sought to understand the mechanisms of DLK-based signaling in the context of nervous system development. Using an in vitro NGF withdrawal paradigm that mimics the competition for trophic factors encountered by peripherally projecting sensory neurons in vivo, we discovered that DLK is required for both axonal degeneration and neuronal apoptosis. DLK-mediated degeneration is based on specific regulation of stress-induced JNK activity in axons that is achieved via interaction of DLK with the scaffolding protein JIP3. These results are further supported by the observation that developmental apoptosis is significantly reduced in multiple neuronal populations in vivo. Collectively, this suggests that DLK-based regulation of the JNK signaling pathway is essential for the neuronal apoptosis and axon degeneration that occur during development.

Results

DLK is required for neuronal apoptosis and axon degeneration in DRG neurons

DLK is specifically expressed in postmitotic neurons during development, including neurons of the DRG and spinal cord (Hirai et al., 2005). We generated DLK-null animals through excision of exons 2–5, which resulted in no expression of DLK protein in the embryonic nervous system (Fig. S1). In the presence of NGF, DRG neurons from DLK$^{-/-}$ mice in culture appeared morphologically normal and displayed comparable growth with neurons from wild-type (wt) littermates, indicating no major defects in axon outgrowth in this neuronal population (Fig. S2). To ascertain whether DLK regulates neuronal apoptosis, we cultured DRG neurons in the presence of NGF to elicit growth and then withdrew NGF from the culture media to induce neuronal degeneration. Levels of apoptosis after NGF withdrawal were measured by counting the number of neuronal cell bodies staining positive with an antibody against the activated form of caspase 3, which is elevated during apoptosis in this cell population. Interestingly, the presence of activated caspase 3 in neuronal cell bodies was strikingly reduced in DLK$^{-/-}$ neurons as compared with controls, indicative of a significant protection of DLK$^{-/-}$ neurons from apoptosis induced by NGF withdrawal (Fig. 1, A–D).

NGF deprivation has also been shown to induce axonal degeneration independent of cell death in NGF-dependent cell populations (Campenot, 1977); therefore, we next explored whether DLK is also required for axon degeneration using DRG explant cultures. Interestingly, whereas axons grown from wt DRG explants completely degenerated by 18 h, DLK-null neurons displayed minimal degeneration at this time point (Fig. 1, E–H). The axonal protection observed in explant cultures could be a secondary result of the antiapoptotic effects of DLK removal, so we next examined whether DLK affects local axon degeneration using compartmentalized chambers that separate axons from cell bodies. When NGF is removed only from the axonal compartment in this experimental setup, degeneration of axons proceeds on a similar timeline to that observed in explants, but no significant apoptosis occurs during this time period (Campenot, 1977; Mok et al., 2009). Similar to what was observed in explants, DLK$^{-/-}$ axons displayed significantly reduced degeneration after NGF deprivation as compared with axons from wt littermates (Fig. 1, I–L). These data argue that DLK is critical for both axon degeneration and cell death in response to growth factor deprivation. Importantly, loss of DLK is also able to protect against local axon degeneration, arguing that it has an essential role in this process even in conditions in which neuronal apoptosis does not occur.

DLK activates a JNK-mediated stress response pathway

To identify pathways modulated by DLK in the context of developmental degeneration in mouse, the activation of MAPK pathways was measured in cultured DRG neurons after 3 h of NGF deprivation. This early time point is before significant degeneration but is sufficient to cause a fourfold reduction in the levels of phosphorylated extracellular signal-regulated kinase (ERK; p-ERK) resulting from the loss of NGF/TrkA-based survival signaling. Levels of p-ERK were similar in wt and DLK$^{-/-}$ neurons, arguing that the removal of DLK does not protect neurons via maintaining ERK activity in the absence of NGF (Fig. 2, A and B). Levels of phosphorylated JNK (p-JNK) and phosphorylated P38-α were unchanged at this time point, though

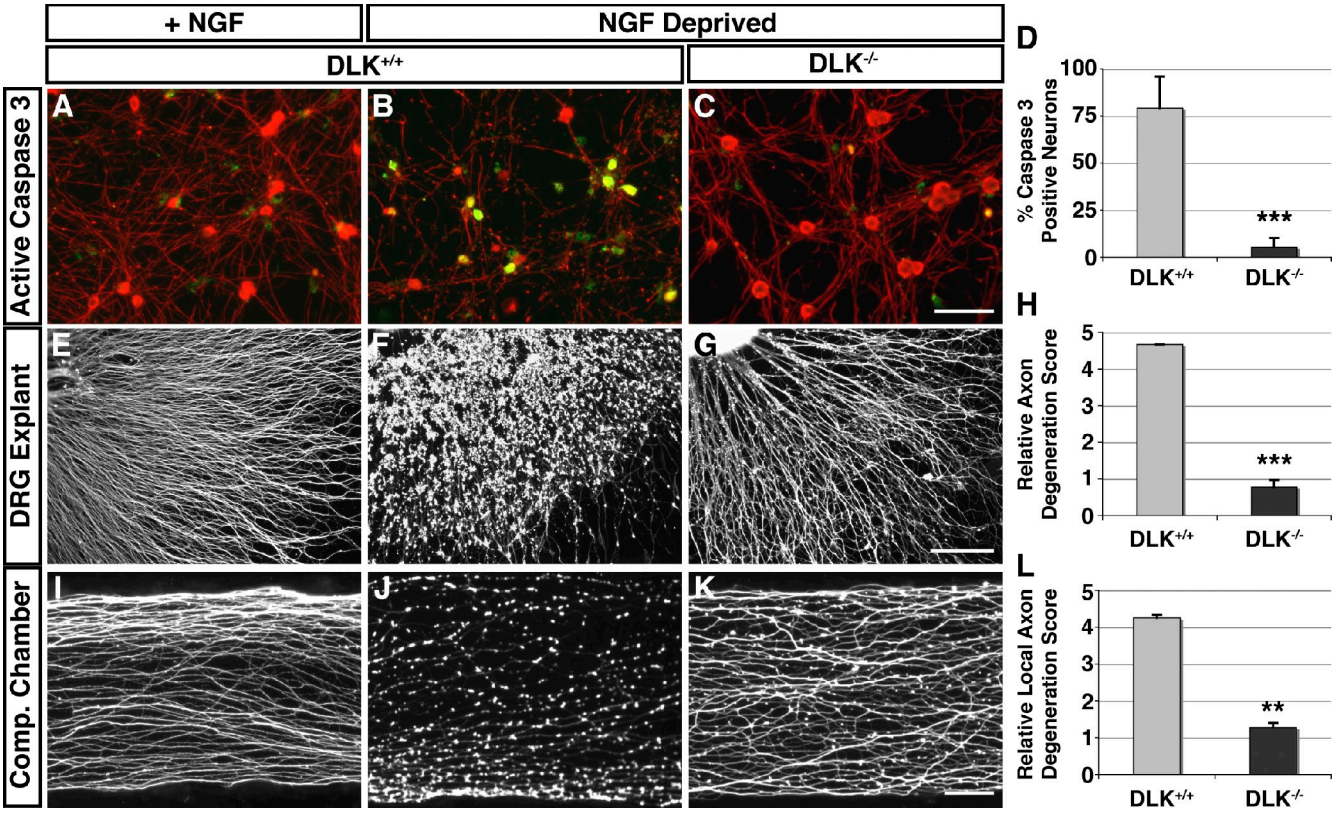

Figure 1. **Apoptosis and axon degeneration are significantly reduced in DLK$^{-/-}$ neurons.** (A–C) Cultured DRG neurons from E13.5 embryos stained with antibodies for activated caspase 3 (green) and Tuj1 (red). Neurons grow robustly in the presence of NGF (A) and display negligible activated caspase 3 staining. Caspase 3 is activated in many neurons after 8 h of NGF withdrawal in wt (DLK$^{+/+}$) neurons (B) but is reduced in DLK$^{-/-}$ neurons (C). Bar, 50 µm. (D) Quantification of cultures shown in A–C reveals significantly less activation of caspase 3 in DLK$^{-/-}$ neurons (wt = 79 ± 17% and DLK$^{-/-}$ = 5 ± 4.5% of neurons; $n = 3$; ***, $P < 0.001$). (E–G) Tuj1 staining of DRG explants from wt and DLK$^{-/-}$ embryos in the presence or absence of NGF. NGF results in robust axon outgrowth from explants (E). Withdrawal of NGF from explant cultures results in the degeneration of axons in a period of 18 h in wt explants (F) but not in DLK$^{-/-}$ explants (G). Bar, 100 µm. (H) Quantification of cultures shown in F and G using a scoring system designed to measure the amount of axon degeneration (0 = no degeneration, and 5 = complete degeneration) reveals significantly less degeneration in DLK$^{-/-}$ axons (wt = 4.7 ± 0.1 and DLK$^{-/-}$ = 0.8 ± 0.2; $n = 5$; ***, $P < 0.001$). (I–K) Tuj1 staining of DRG axons from E13.5 embryos from wt and DLK$^{-/-}$ embryos grown in compartmentalized (Comp.) chambers that separate distal axons from cell bodies. NGF elicits robust growth (I), and removal of NGF from the axonal compartment only results in rapid local degeneration of wt axons (J) but not DLK$^{-/-}$ axons (K) in 28 h. Bar, 50 µm. (L) Quantification of compartmentalized chamber cultures shown in J and K using the aforementioned scoring system reveals reduced axon degeneration in DLK$^{-/-}$ (wt = 4.25 ± 0.1 and DLK$^{-/-}$ = 1.3 ± 0.1; $n = 2$; **, $P < 0.01$). Error bars represent SEM.

examination of p-JNK 1 h after NGF withdrawal revealed that levels were increased roughly threefold over controls at this early time point. This increase was largely absent in DLK$^{-/-}$ neurons, where levels increased only 1.4 fold after NGF deprivation. A more thorough time course revealed that, after the transient increase in p-JNK at 1 h, levels remained similar to control through 9 h in wt neurons but were not elevated in DLK$^{-/-}$ neurons at any time point examined (Fig. S3). Phosphorylated c-Jun (p-c-Jun) levels were also significantly elevated beginning 3 h after NGF deprivation in wt neurons and extending until the onset of degeneration, an increase that was absent in DLK$^{-/-}$ neurons (Figs. 2 [A and B] and S3). These data suggest that the withdrawal of NGF induces JNK-based stress response pathways in DRG neurons and that this activation is DLK dependent.

To better understand the mechanism of JNK activation induced by NGF withdrawal, we next examined p-JNK localization by immunostaining to determine the subcellular distribution of p-JNK protein. Under normal culture conditions, DRG neurons showed punctate p-JNK staining throughout the cell body and neuronal processes in both wt and DLK$^{-/-}$ neurons (Figs. 2 [C and D] and S3). Interestingly, NGF deprivation resulted in a redistribution of p-JNK from axons to cell bodies over a period of 4 h, which did not occur in DLK$^{-/-}$ neurons (Figs. 2 [E and F] and S3). Staining of cultures with an antibody directed to Tuj1 confirmed that the lack of p-JNK labeling in axons was not a result of the axons degenerating but rather a specific relocalization of p-JNK to the cell body (Fig. 2, G and H). The timing of p-JNK relocalization strongly correlated with the number of neurons that stained positive for p-c-Jun (Fig. 2, I–K), consistent with the hypothesis that nuclear localization of p-JNK is required for c-Jun phosphorylation and neuronal apoptosis (Björkblom et al., 2008).

To define the functional role of the increased JNK activity observed in DRG neurons as a consequence of NGF withdrawal, we tested the effect of JNK inhibitors on NGF withdrawal–induced degeneration. Pharmacological inhibition of JNK activity was sufficient to significantly reduce levels of caspase 3 activation observed in dissociated DRG cultures (Fig. 3, A–C) and rescue axons from degeneration (Fig. 3, D–F) induced by NGF deprivation. These protective effects were similar to those

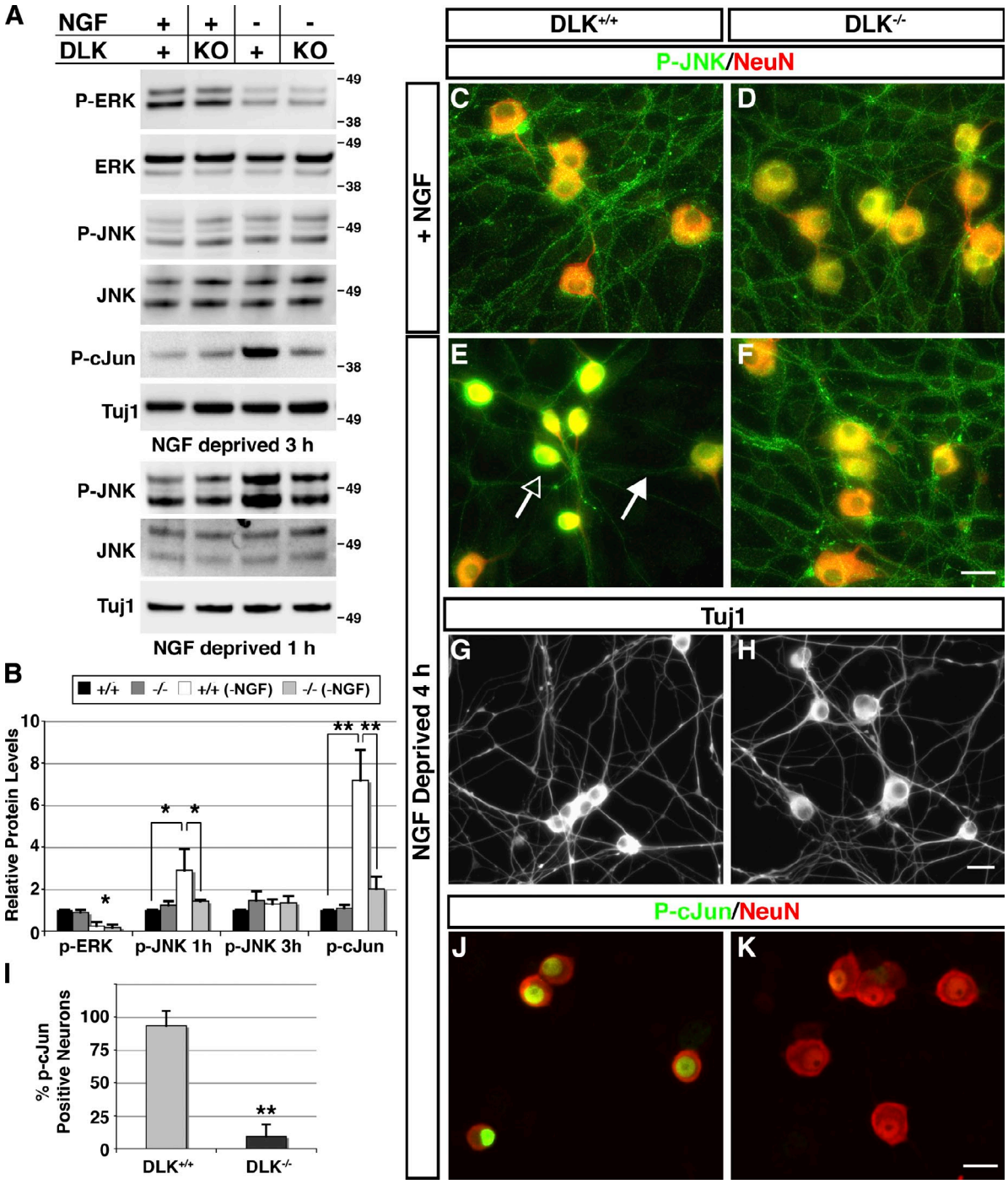

Figure 2. **DLK is required for activation of stress-induced JNK signaling in neurons but does not affect basal JNK activity.** (A and B) Phosphorylation levels of ERK, JNK, and c-Jun in E13.5 DRG neuron cultures from wt ($DLK^{+/+}$) and $DLK^{-/-}$ embryos in the presence or absence of NGF by Western blotting (A). Quantification of A reveals that levels of p-ERK are reduced in both $DLK^{-/-}$ and wt neurons 3 h after NGF withdrawal (wt = 26.2 ± 19% and $DLK^{-/-}$ = 19.1 ± 13% of NGF control; $n = 4$; *, $P < 0.05$), whereas no change in p-JNK is observed at this time point. At 1 h, p-JNK levels are increased in wt neurons but not $DLK^{-/-}$ neurons after NGF withdrawal (wt = 289 ± 100% and $DLK^{-/-}$ = 143 ± 16% of NGF control; $n = 4$; $P < 0.05$). wt neurons displayed a large increase in p-c-Jun 3 h after NGF withdrawal, which is significantly reduced in $DLK^{-/-}$ neurons (wt = 717 ± 146% and $DLK^{-/-}$ = 201 ± 58% of NGF control; $n = 4$; **, $P < 0.01$; B). Molecular mass is indicated in kilodaltons. (C–F) Cultured DRG neurons from E13.5 embryos stained with antibodies for activated p-JNK and NeuN. p-JNK is largely relocalized from the axon (white arrow) to the nucleus (open arrow) after 4 h of NGF withdrawal in wt neurons but not in $DLK^{-/-}$ neurons. (G and H) DRG neurons stained with Tuj1 show that loss of p-JNK in axons is not a result of axonal degeneration at this time point. (I) Quantification of cultures shown in J and K reveals significantly less p-c-Jun staining in $DLK^{-/-}$ neurons (wt = 93 ± 11.5% and $DLK^{-/-}$ = 9 ± 9% of neurons; $n = 2$; **, $P < 0.01$). (J and K) DRG neurons stained with activated p-c-Jun and NeuN. In wt cultures, the majority of neurons are p-c-Jun positive after 4 h of NGF withdrawal, whereas in $DLK^{-/-}$ cultures, only a few neurons show dim staining for p-c-Jun. Error bars represent SEM. Bars, 10 µm.

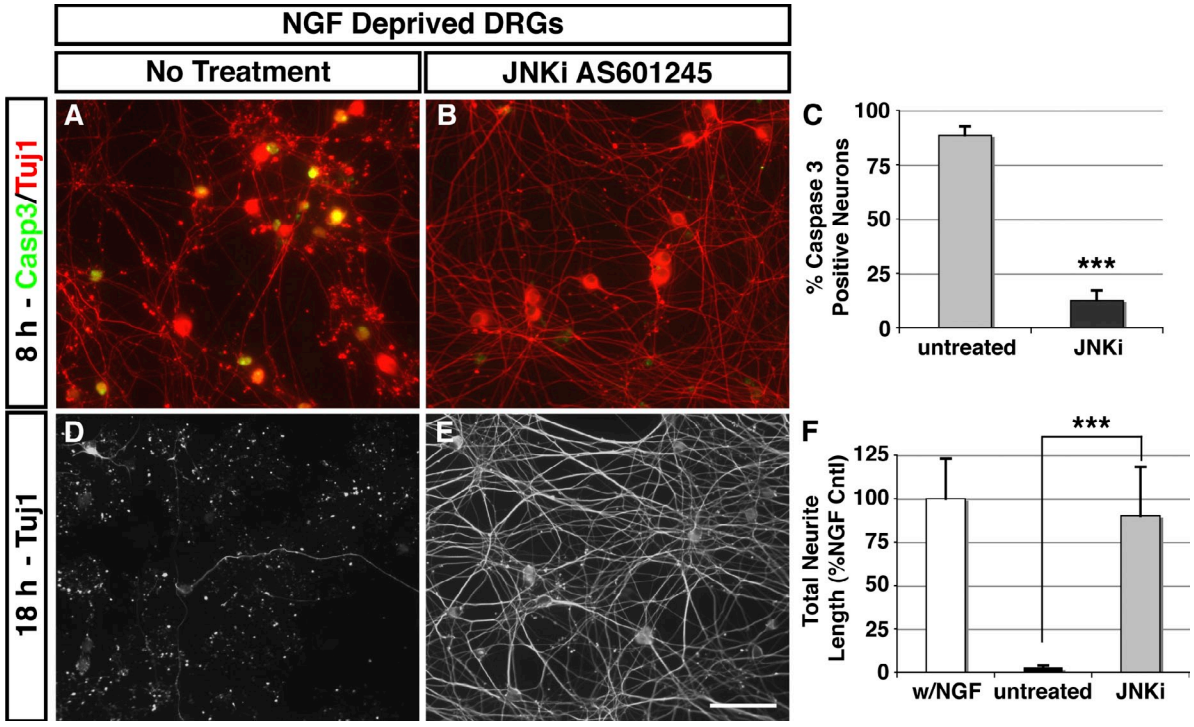

Figure 3. **Inhibition of JNK activity protects DRG neurons from degeneration.** (A and B) DRG neurons from E13.5 embryos stained with antibodies for activated caspase 3 (Casp3) and Tuj1 after 8 h of NGF withdrawal. Caspase 3 is activated in many untreated neurons (A), but fewer neurons treated with the JNK inhibitor (JNKi) AS601245 displayed caspase activation (B). (C) Quantification of cultures shown in A and B reveals significantly less activation of caspase 3 in neurons treated with JNK inhibitor AS601245 (untreated = 89 ± 4.1% and JNK inhibitor = 12 ± 4.5% of neurons; $n = 3$; ***, $P < 0.001$). (D and E) DRG neurons from wt E13.5 embryos after 18 h of NGF withdrawal and stained with Tuj1. Untreated neurons were completely degenerated (D), whereas neurons treated with the JNK inhibitor AS601245 did not show significant degeneration (E). Bar, 50 µm. (F) Quantification of the total neurite length in the culture shown in D and E reveals significant inhibition of degeneration in the presence of JNK inhibitor AS601245 (untreated = 2.9 ± 0.9% and JNK inhibitor = 90 ± 28% of NGF control [Cntl; w/NGF]; $n = 3$; ***, $P < 0.001$). Error bars represent SEM.

observed in DLK$^{-/-}$ neurons (Fig. 1, A–H). As small molecule inhibitors can often inhibit multiple kinases in addition to their desired target, this experiment was repeated with two additional structurally distinct JNK inhibitors, which yielded similar results (SP600125 and JNK VIII; unpublished data). These data support a mechanism in which DLK is required for activation of the JNK–c-Jun stress response pathway that occurs in neurons as a result of NGF deprivation, and this JNK activity results in neuronal apoptosis and degeneration of axons.

Selective activation of JNK by DLK requires JIP3

The observation that DLK$^{-/-}$ neurons retain normal localization and levels of p-JNK when cultured in the presence of NGF, yet display deficiencies in p-JNK relocalization and attenuated phosphorylation of c-Jun in NGF deprivation paradigms, suggested that DLK is able to selectively modulate the prodegenerative aspects of JNK signaling. We hypothesized that this may be achieved through the interaction of DLK with a specific JIP to form a signaling complex that would allow for restricted JNK activation. To test this possibility, we examined whether siRNA-based knockdown of individual JIPs was able to phenocopy the protective effects observed in DLK$^{-/-}$ neurons. Interestingly, siRNA-based knockdown of JIP3 provided similar levels of protection to those observed after knockdown or knockout of DLK, whereas JIP1 siRNAs provided negligible protection despite efficient knockdown of JIP1 protein (Figs. 4 [A–G] and S4).

To determine whether JIP3 and DLK can form a signaling complex, we tested whether these two proteins interact when coexpressed in HEK-293 cells. Immunoprecipitation (IP) of Flag-tagged DLK was able to pull down coexpressed Myc-tagged JIP3 but not a GFP control (Fig. 4 H), indicating that these proteins can interact. To investigate whether this JIP3–DLK complex was functionally relevant, we next assessed the ability of JIP3 to enhance the DLK-dependent activation of JNK and c-Jun. Transfection of DLK into HEK-293 cells resulted in increased phosphorylation of JNK and c-Jun, even in the absence of any extrinsic stress on these cells (Fig. 4 I). This phosphorylation did not occur after transfection of a kinase-dead DLK construct, arguing that it is a specific signaling event (unpublished data). Transfection of JIP3 alone did not result in significant phosphorylation of JNK, but when JIP3 was cotransfected with DLK, it resulted in notably higher levels of p-JNK and p-c-Jun than DLK alone (Fig. 4 I). This demonstrates that DLK activity is sufficient to stimulate the phosphorylation of JNK, and JIP3 enhances this activation.

To determine whether a DLK–JIP3 complex regulates stress-induced JNK activity in neurons, we next examined whether the endogenous DLK and JIP3 genes interact as was observed after overexpression in HEK-293 cells. Sufficient protein for IP studies could not be obtained from DRG neurons,

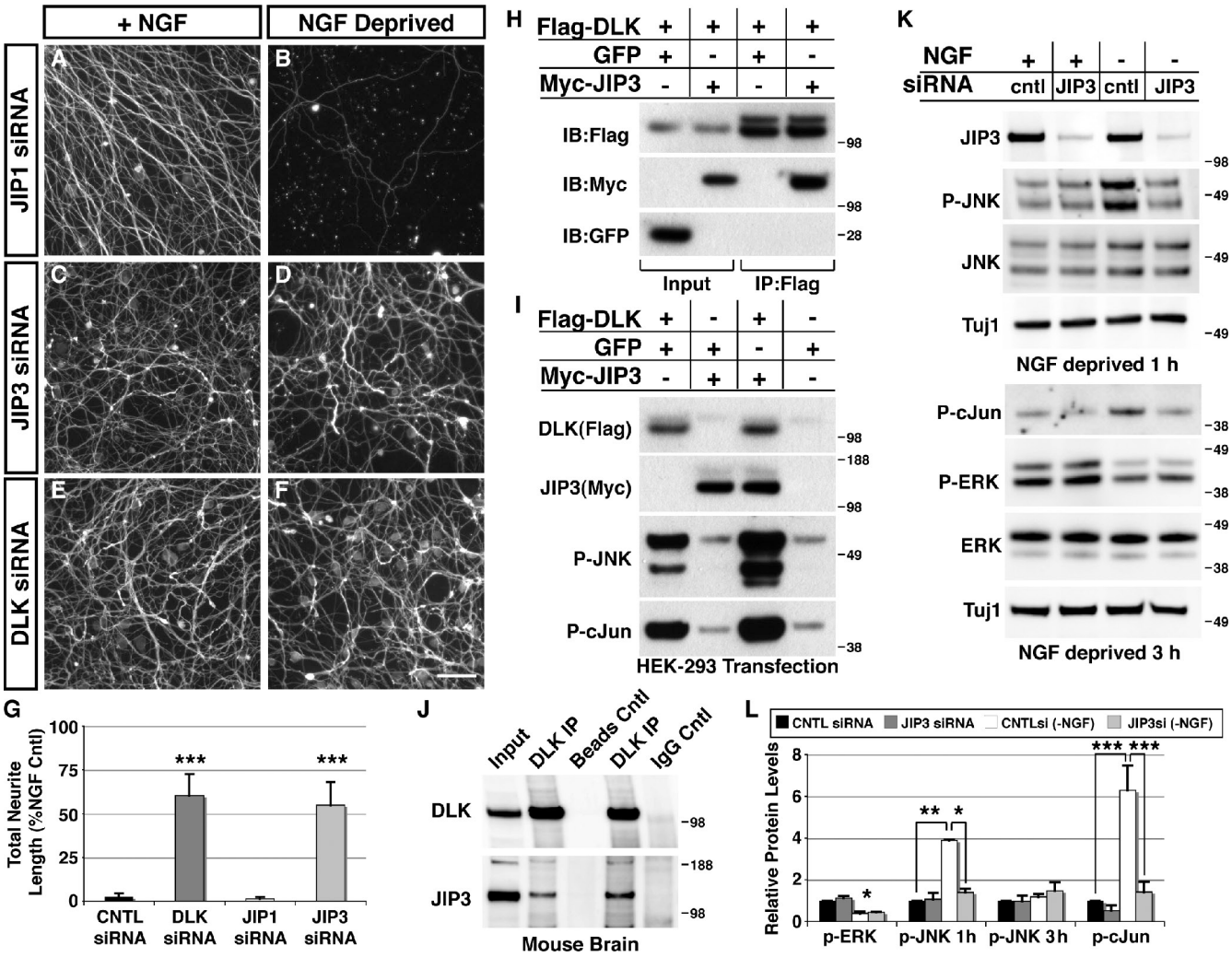

Figure 4. **JIP3 is required for neuronal degeneration and forms a complex with DLK, which regulates neuronal JNK activity.** (A–F) Tuj1 staining of DRG neurons from E13.5 embryos electroporated with various siRNAs and cultured in the presence of NGF or after 18 h of NGF withdrawal. An siRNA against JIP1 (A and B) did not protect neurons from degeneration, whereas siRNAs against JIP3 (C and D) or DLK (E and F) provided significant protection from degeneration. Bar, 50 µm. (G) Quantification of the total neurite length in the cultures shown in A–F reveals that siRNAs directed against either JIP3 or DLK provide significant protection against NGF withdrawal–induced degeneration (control [CNTL] = 2.6 ± 1.9%, DLK = 61 ± 12%, JIP1 = 1.3 ± 1.2%, and JIP3 = 55 ± 13%; $n > 3$; ***, $P < 0.001$) (H) A Western blot for Flag-DLK and Myc-JIP3 after IP of Flag-DLK from cotransfected HEK-293 cells. Myc-JIP3 but not GFP is pulled down with Flag-DLK when the two proteins are coexpressed. IB, immunoblot. (I) A Western blot for p-JNK and p-c-Jun after transfection of DLK and/or JIP3 in HEK-293 cells. Transfection of DLK in the absence of stress results in increases in p-JNK and p-c-Jun. Transfection of JIP3 alone does not activate p-JNK or p-c-Jun, yet cotransfection of DLK and JIP3 results in more JNK and c-Jun phosphorylation than transfection of DLK alone. (J) A Western blot for DLK and JIP3 after IP from neonatal mouse brain using an anti-DLK antibody. Both proteins are pulled down by the anti-DLK antibody but not in control experiments using no antibody (Beads Cntl) or an IgG control (IgG Cntl). (K and L) Phosphorylation levels of ERK, JNK, and c-Jun in E13.5 DRG neuron cultures electroporated with either a control siRNA or a JIP3 siRNA by Western blotting (K). Quantification of K reveals that levels of p-ERK are reduced in both control and JIP3-treated neurons 3 h after NGF withdrawal (control = 39 ± 10%, JIP3 = 44 ± 9.5%; $n = 3$; *, $P < 0.05$), whereas no change in p-JNK is observed at this time point. At 1 h, p-JNK levels are increased in control neurons but not JIP3-treated neurons after NGF withdrawal (control = 390 ± 4.2%, JIP3 = 119 ± 18%; $n = 3$; **, $P < 0.01$). Control neurons displayed an even larger increase in p-c-Jun 3 h after NGF withdrawal, which is significantly reduced in JIP3-treated neurons (control = 629 ± 118% and JIP3 = 141 ± 49%; $n = 3$; ***, $P < 0.001$; L). The control is an siRNA directed against luciferase. Molecular mass is indicated in kilodaltons. Error bars represent SEM.

so whole-brain lysate from neonatal mice (postnatal day 1) was used as a substitute. Consistent with our previous observations, IP with an anti-DLK antibody was also able to pull down JIP3 protein, which was not observed in an IgG control (Fig. 4 J). The functional relevance of this interaction was then examined by measuring the phosphorylation of JNK, c-Jun, and ERK in DRGs after siRNA knockdown of JIP3 in the presence or absence of NGF. The results observed were nearly identical to those observed with $DLK^{-/-}$ neurons, i.e., the increase in levels of p-c-Jun seen in control cultures was not observed in neurons electroporated with a JIP3 siRNA after 3 h of NGF deprivation, and the modest increase in p-JNK at 1 h was not observed after JIP3 knockdown (Fig. 4, K and L). siRNA-based knockdown of JIP3 also inhibited relocalization of p-JNK in dissociated DRG cultures (unpublished data). Although these data cannot distinguish between a direct JIP3–DLK interaction and one that requires additional binding partners, it strongly suggests that DLK and JIP3 are components of a signaling complex that is required for JNK and c-Jun phosphorylation induced by NGF withdrawal.

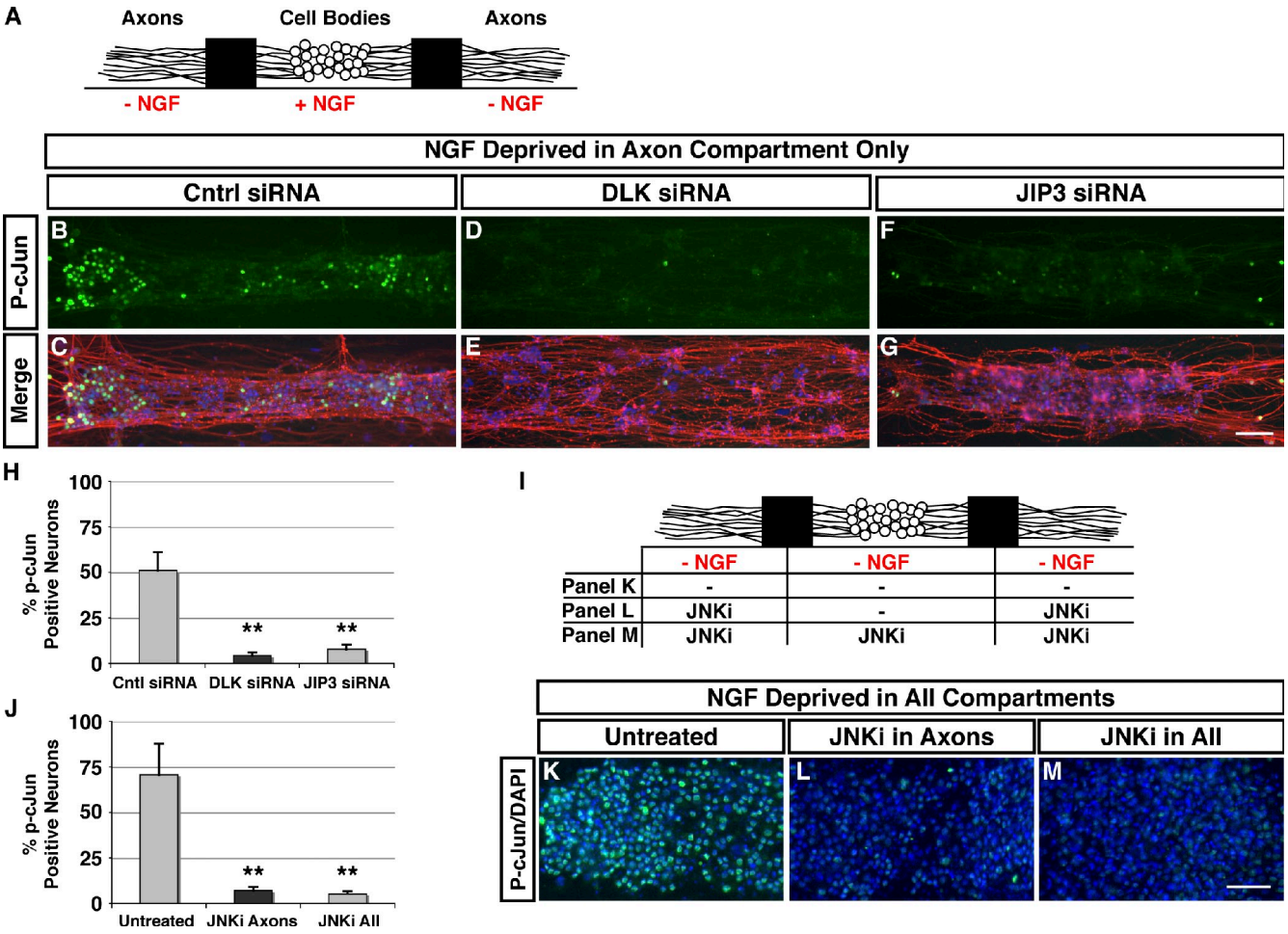

Figure 5. **DLK, JIP3, and JNK are components of a peripherally derived stress signal that regulates c-Jun phosphorylation.** (A) A schematic of an experiment using compartmentalized culture chambers shown in B–G in which NGF is removed from distal axons only, and levels of p-c-Jun are visualized in the central chamber containing cell bodies. (B–G) A central compartment of culture chamber containing DRG neurons stained with p-c-Jun (green in B, D, and F) or p-c-Jun merged with DAPI (blue) and Tuj1 (red) after 6 h of NGF withdrawal from distal axons (C, E, and G). Neurons electroporated with a control (Cntrl) siRNA show many p-c-Jun–labeled neurons (B and C), whereas neurons electroporated with siRNAs directed to DLK (D and E) or JIP3 (F and G) have fewer p-c-Jun–positive nuclei. Bar, 50 µm. (H) Quantification of the percentage of p-c-Jun–positive cells shown in B–G after NGF withdrawal from distal compartments (control [Cntl] = 51.0 ± 10%, JIP3 = 7.7 ± 2.4%, and DLK = 4.3 ± 1.7%; **, $P < 0.01$). (I) A schematic of an experiment shown in K–M in which NGF is removed from all compartments, and the JNK inhibitor (JNKi) AS601245 is added only to the distal axon compartments or all compartments. (J) Quantification of p-c-Jun–labeled cells after NGF withdrawal ± JNK inhibitors in different compartments (untreated = 70.6 ± 17%, axons = 7.8 ± 2%, and all = 5.2 ± 1.4%; **, $P < 0.01$). (H and J) $n = 2$. Error bars represent SEM. (K–M) Staining of DRG cell bodies for p-c-Jun (green) and DAPI (blue) 6 h after NGF withdrawal (K). The addition of the JNK inhibitor to the distal axon compartment alone results in minimal c-Jun phosphorylation after NGF withdrawal from all compartments (L). The addition of the JNK inhibitor to all compartments also inhibits c-Jun activation (M). Bar, 50 µm.

DLK activation in distal axons initiates a retrograde stress response

Our previous work demonstrated that a significant portion of DLK protein was localized to the growth cone in projecting axons (Lewcock et al., 2007). This raises the possibility that regulation of neuronal apoptosis by DLK originates in the periphery and is retrogradely transported back to the nucleus. To test this hypothesis, we again used DRG neurons grown in compartmentalized culture chambers to separate axons from cell bodies (Fig. 5 A). In this setup, removal of NGF selectively from distal axons does not result in rapid neuronal apoptosis but is sufficient to induce phosphorylation of c-Jun in the nucleus within 6 h, a similar timeline to what is observed in dissociated cultures (Fig. 5, B and C; Mok et al., 2009). Interestingly, when this experiment was conducted in neurons electroporated with siRNAs directed against either DLK or JIP3 before plating, a significant reduction in the number of p-c-Jun–positive cells was observed (Fig. 5, D–H), arguing that the DLK–JIP3 signaling complex is essential for c-Jun phosphorylation. Experiments using siRNA-based knockdown were unable distinguish between DLK–JIP3 acting in the distal axon or in the central compartment in response to a distinct peripherally derived signal. To address this, a complementary experiment was performed in which NGF was removed from all compartments, and JNK inhibitors were added to the distal axons only (Fig. 5 I). JNK inhibitors used as specific inhibitors of DLK were not available, and our data suggest that DLK-induced degeneration is mediated largely by JNK (Fig. 3). Removal of NGF from all compartments of the chamber results in neuronal apoptosis equivalent to that seen in dissociated cultures (Mok et al., 2009) and allows assessment of whether inhibition of DLK–JNK in the distal axon is sufficient to prevent cell death. We again

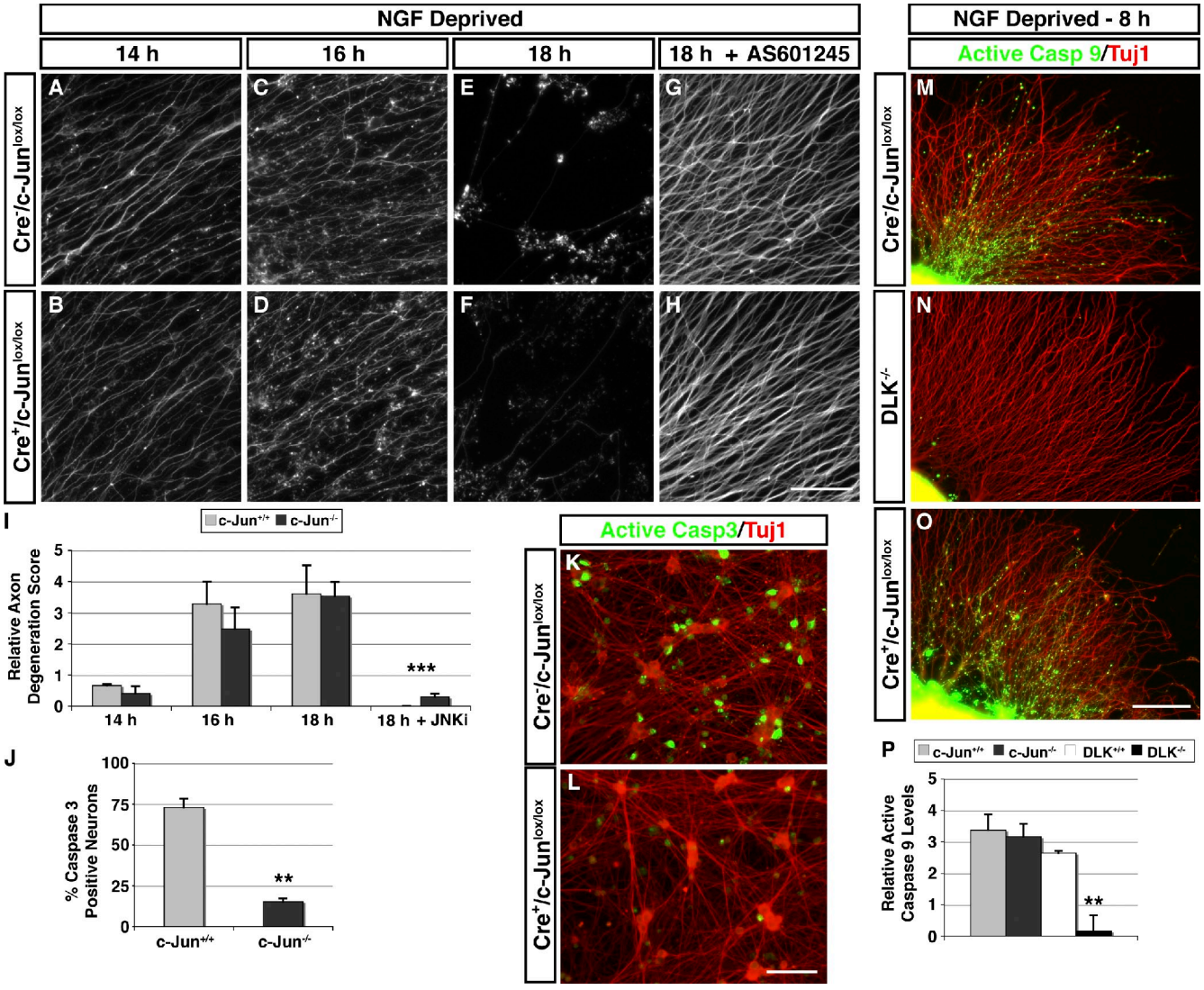

Figure 6. **DLK–JNK-dependent regulation of axon degeneration is independent of c-Jun.** (A–F) Tuj1 staining of axons from wt (c-Jun$^{lox/lox}$ and Cre negative) and c-Jun$^{lox/lox}$ DRG explants after 14 (A and B), 16 (C and D), or 18 (E and F) h of NGF withdrawal. (G and H) Tuj1 staining of axons from wt and c-Jun$^{lox/lox}$ DRG explants treated with JNK inhibitor AS601245 after 18 h of NGF withdrawal. (A–H) Bar, 25 µm. (I) Quantification of explants shown in A–H reveals that degeneration of c-Jun$^{lox/lox}$ axons is comparable with wt controls, but the addition of a JNK inhibitor (JNKi) provides significant protection in both genotypes (18-hr axon degeneration score: wt = 3.6 ± 0.9, c-Jun$^{lox/lox}$ = 3.5 ± 0.4, wt + JNKi = 0 ± 0, and c-Jun$^{lox/lox}$ + JNKi = 0.3 ± 0.1; n = 5; ***, P < 0.001). (J) Quantification of caspase 3 staining shown in K and L reveals significantly less active caspase 3–positive c-Jun$^{lox/lox}$ neurons compared with wt littermates (wt = 73 ± 5.3% and c-Jun$^{lox/lox}$ = 15 ± 2.2% of neurons; n = 3; **, P < 0.01). (K and L) DRG neurons from E13.5 embryos stained with antibodies for activated caspase 3 (Active Casp2) and Tuj1 after 8 h of NGF withdrawal. Caspase 3 is activated in many wt neurons after 8 h of NGF withdrawal (K) but in fewer c-Jun$^{lox/lox}$ neurons (L). Bar, 50 µm. (M–O) DRG explants from wt, DLK$^{-/-}$, and c-Jun$^{lox/lox}$ stained for activated caspase 9 and Tuj1. Caspase 9 is activated in many axons after 8 h of NGF withdrawal in wt and c-Jun$^{lox/lox}$ neurons (M and O), but no activation is observed in DLK$^{-/-}$ neurons (N). Bar, 100 µm. (P) Quantification of active caspase 9 in DRG explants from DLK$^{-/-}$, c-Jun$^{lox/lox}$, and controls shown in M–O reveals significantly less activation of caspase 9 in DLK$^{-/-}$ axons as compared with wt and c-Jun$^{lox/lox}$ DRG axons (c-Jun$^{lox/lox}$ = 3.2 ± 0.4 and DLK$^{-/-}$ = 0.2 ± 0.3; n = 3; **, P < 0.01). Error bars represent SEM.

examined p-c-Jun levels as a readout, as previous studies have shown that it is an essential step toward neuronal apoptosis under conditions of global NGF deprivation (Ham et al., 1995; Whitfield et al., 2001; Palmada et al., 2002). Interestingly, the addition of JNK inhibitors to distal axons alone was able to significantly reduce numbers of p-c-Jun–positive cells in the central compartment to levels similar to those seen when JNK inhibitors were added to all compartments (Fig. 5, J–M). These observations suggest that DLK–JNK activity in distal axons is necessary though not sufficient for NGF withdrawal–induced apoptosis.

JNK but not c-Jun is required for axonal degeneration

Next, we addressed whether regulation of axon degeneration by DLK is also c-Jun dependent. To do this, we measured levels of axon degeneration in c-Jun conditional–null mice crossed to a Nestin-Cre (Behrens et al., 2002), which eliminates c-Jun expression in nearly all DRG neurons by E13.5 (embryonic day 13.5; abbreviated c-Jun$^{lox/lox}$; unpublished data). NGF was withdrawn from explants for 14, 16, or 18 h to assess the rate of axon degeneration in each genotype. Surprisingly, axons from c-Jun$^{lox/lox}$ explants degenerated at similar rates to axons

from wt or heterozygous littermates (Fig. 6, A–F and I). However, when JNK inhibitors were added to c-Jun$^{lox/lox}$ explants during NGF deprivation, a strong protection of axons was observed (Fig. 6, G–I). To confirm that the loss of c-Jun is sufficient to rescue neuronal apoptosis of DRG neurons, we examined the activation of caspase 3 in neuronal cell bodies after the removal of NGF. Consistent with previous studies in sympathetic neurons (Ham et al., 1995; Palmada et al., 2002), a significantly reduced number of c-Jun$^{lox/lox}$ neurons stained with an antibody specific for the activated form of caspase 3 (Fig. 6, K and L). This implies that, although c-Jun is essential for neuronal apoptosis after NGF withdrawal, downstream targets of JNK activity other than c-Jun regulate axon degeneration after NGF deprivation.

Activation of caspases is downstream of JNK–c-Jun activity in apoptosis of sympathetic neurons (Whitfield et al., 2001) and has more recently been demonstrated to be essential for axon degeneration in the context of NGF withdrawal (Nikolaev et al., 2009; Schoenmann et al., 2010). Based on these findings, we sought to determine whether caspases were activated in DLK$^{-/-}$ axons. To do this, we monitored the activity of caspase 9, as this is the primary initiator caspase in the intrinsic cell death pathway and downstream of BAX, which is also required for axon degeneration (Nikolaev et al., 2009). Using a cleaved caspase 9–specific antibody, activation of this protease could be observed after 8 h of NGF withdrawal in axons of wt explant cultures, but no activation was observed in axons of DLK$^{-/-}$ explants, indicating that DLK is upstream of axonal caspase activity (Fig. 6, M–P). To determine whether c-Jun is required downstream of DLK for caspase 9 activation, we conducted a similar experiment using c-Jun$^{lox/lox}$ neurons. Consistent with the timeline of degeneration observed in c-Jun$^{lox/lox}$ explants, c-Jun$^{lox/lox}$ axons had similar levels of active caspase 9 present in axons as compared with wt control cultures (Fig. 6, M and O), whereas treatment of wt cultures with JNK inhibitors yielded similar levels of caspase 9 activation to what was seen in DLK$^{-/-}$ neurons (not depicted). This suggests that, unlike what has been reported in the context of neuronal apoptosis after NGF withdrawal, caspase activation and subsequent degeneration of axons are not dependent on c-Jun transcriptional activity.

DLK is required for developmental apoptosis in vivo

To determine the relevance of DLK for neuronal apoptosis and axon degeneration in normal development, we examined the phenotype of DLK$^{-/-}$ mice during the period of axon projection and refinement in DRG neurons (E12.5–17.5). At E12.5, a developmental stage before any significant developmental apoptosis in DRG neurons (White et al., 1998), DLK-null mice were grossly indistinguishable from wt littermates and displayed normal patterns of motor and sensory axon outgrowth in vivo, consistent with our in vitro observations (Fig. S5). However, examination of E17.5 embryos revealed notable increases in the number of DRG neurons in DLK-null animals, with a 1.8-fold increase in the total number of pan-Trk–stained DRG neurons compared with wt littermates in the lumbar region (Fig. 7, A–C). When the number of pan-Trk–stained neurons was normalized to the total DRG area, a 1.5-fold increase in neuronal number/DRG area was still observed in DLK$^{-/-}$ embryos, indicative of more neurons being packed into individual DRGs (Fig. 7 D). The phenotype of DLK$^{-/-}$ neurons we observed in culture suggested that the increase in Trk-positive cell number observed at later stages was likely a result of reduced developmental apoptosis in DLK$^{-/-}$ embryos. To test this hypothesis, E15.5 embryos were stained for the activated form of caspase 3, which revealed a 1.7-fold decrease in the amount of cells per area undergoing apoptosis in DLK$^{-/-}$ DRGs as compared with wt littermate controls (Fig. 7, E–G). We were unable to identify in vivo axon degeneration phenotypes in DRG neurons as a result of two main limitations. First, no measurable axonal degeneration/pruning events in DRG neurons have been identified that occur in the absence of a secondary mutation (Schoenmann et al., 2010). Second, it would be impossible to discriminate between true axon degeneration defects and axonal misprojection as a result of excess DRG neurons in DLK$^{-/-}$ mice.

DLK is broadly expressed in the nervous system, so we next examined whether reductions in developmental apoptosis also occurred in spinal motor neurons, another neuronal population in which excess neurons are lost between E13.5 and 17.5 (White et al., 1996, 1998). To do this, we stained lower thoracic spinal cord sections from DLK$^{-/-}$ mice with an antibody to HB9, a spinal motor neuron–specific marker (Arber et al., 1999). Normal numbers of HB9-positive motor neurons were present in DLK$^{-/-}$ embryos at E13.5, yet by E15.5, the number of motor neurons in DLK$^{-/-}$ embryos was roughly double that of wt littermates (186% of control; Fig. 7, H–K and N). This increase in cell number was sustained at E17.5, the latest time point examined as a result of neonatal lethality of DLK-null animals (180% of control; Fig. 7, L–N). As initial numbers of motor neurons were generated in DLK$^{-/-}$ embryos, this phenotype is likely a result of reduced developmental apoptosis in motor neurons during later stages of development, similar to what was observed in DRGs. In addition, our results are comparable with changes in the motor neuron cell number observed in animals lacking choline acetyltransferase or BAX, both of which also display defects in developmental loss of motor neurons at similar developmental stages (White et al., 1998; Brandon et al., 2003). Collectively, these data suggest that DLK-dependent signaling pathways are essential to developmental apoptosis in multiple neuronal types.

Discussion

DLK is required for neuronal degeneration during development

In this study, we identify a role for DLK as a critical regulator of neuronal degeneration in multiple peripherally projecting neurons during development. DLK functions in this context by activating JNK-based stress response signaling in a JIP3-dependent fashion without affecting basal JNK activity. The phenotypes observed in DLK$^{-/-}$ mice suggest that DLK is essential for prodegeneration signaling in response to developmental cues in

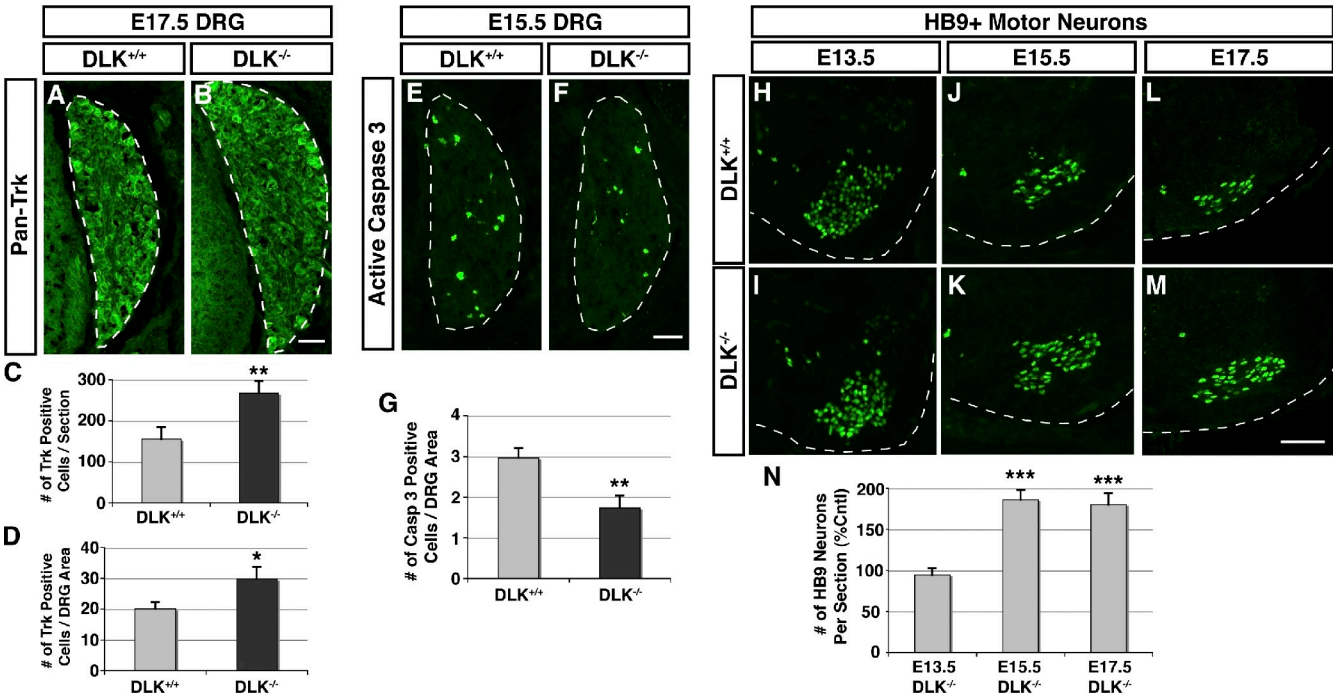

Figure 7. **Developmental loss of DRG and motor neurons is reduced in DLK$^{-/-}$ embryos.** (A and B) Immunohistochemical staining of lumbar level DRGs from E17.5 DLK$^{-/-}$ and wt (DLK$^{+/+}$) littermates with a pan-Trk antibody. DLK$^{-/-}$ DRGs (B) appear larger and contain more Trk-positive neurons than wt controls (A). The border of the DRG is indicated by the dotted lines. Bar, 25 µm. (C) Quantification of pan-Trk staining of DRGs shown in A and B. Significantly more Trk-positive cells per section are present in DRGs of DLK$^{-/-}$ DRGs as compared with wt controls (wt = 155 ± 29 and DLK$^{-/-}$ = 267 ± 31 cells/section; *n* = 3; **, P < 0.01). (D) Normalization of Trk-positive cells to DRG area also showed an increase in the number of neurons in DLK$^{-/-}$ DRGs as compared with wt (wt = 2.0 ± 0.23 and DLK$^{-/-}$ = 2.98 ± 0.39 cells/DRG area; *n* = 3; *, P < 0.05). (E and F) Immunohistochemical staining of lumbar level DRGs from E15.5 DLK$^{-/-}$ and wt (DLK$^{+/+}$) littermates with an antibody specific for active caspase 3. The border of the DRG is indicated by the dotted lines. DLK$^{-/-}$ DRGs (F) have less active caspase 3 staining than wt controls (E). Bar, 25 µm. (G) Quantification of active caspase (Casp) 3–positive cells in DRGs normalized to DRG area at E15.5 reveals a decreased number of active caspase 3–positive cells in DLK$^{-/-}$ embryos (wt = 2.96 ± 0.24 and DLK$^{-/-}$ = 1.73 ± 0.31 cells/DRG area; *n* = 5; **, P < 0.01). (H–M) Immunohistochemical staining with antibodies directed against the motor neuron marker HB9 in thoracic level spinal cords of DLK$^{-/-}$ and wt (DLK$^{+/+}$) littermates at E13.5, 15.5, and 17.5. DLK$^{-/-}$ spinal cords have more HB9-positive cells than wt controls at E15.5 and 17.5. The edge of the spinal cord is indicated by the dotted lines. Bar, 25 µm. (N) Quantification of HB9-positive neurons reveals an equal number of labeled cells in DLK$^{-/-}$ and wt (DLK$^{+/+}$) at E13.5 but a significant increase in the number of labeled cells at E15.5 and 17.5 (E13.5 = 94 ± 8.1%, E15.5 = 186 ± 11%, and E17.5 = 180 ± 14% of wt control [Cntl]; *n* = 3; ***, P < 0.001). Error bars represent SEM.

both motor and sensory neurons. Previous work has established that 50–60% of motor neurons are lost by apoptosis during development (Oppenheim, 1991); therefore, the near doubling of DRG and motor neurons observed in DLK$^{-/-}$ mice implies that these embryos lose few neurons during this time period. This level of protection is surprising, given the amount of cross talk that is often observed within MAPK pathways. Multiple MAPKKKs have been shown capable of activating JNK via MKK4/MKK7 in various contexts (Xu et al., 2001), which leads to the prediction that stress-induced JNK activation would still occur in the absence of a single gene within the pathway. The fact that this does not appear to be the case in DLK$^{-/-}$ embryos could be attributable to many factors, including expression levels within neurons, specific DLK-interacting proteins, or localization of DLK protein to sites within the distal axon where stress is first encountered. Additional studies will be required to discriminate between these possibilities. DRG neurons from DLK$^{-/-}$ embryos do eventually degenerate in our in vitro experimental conditions after longer periods of NGF withdrawal (>72 h; unpublished data). This is in contrast to what was observed in BAX-null neurons, which continue to survive for prolonged periods in the absence of NGF (Deckwerth et al., 1996). This implies that neurons are eventually able to circumvent DLK to initiate degeneration either using a different MAPKKK or via a completely distinct pathway. Nevertheless, the extent of protection observed in DLK$^{-/-}$ mice in vivo indicates that DLK-dependent degeneration is a major neuronal degeneration pathway used during development.

Mechanisms of DLK-dependent degeneration

Our data suggest that DLK regulates neuronal degeneration largely via modulation of the JNK signaling pathway. In contrast to many other cell types, neurons maintain relatively high levels of active JNK even in the absence of stress (Coffey et al., 2000). This high level of p-JNK does not lead to the phosphorylation of proapoptotic downstream targets such as c-Jun and has been hypothesized to phosphorylate a distinct set of downstream targets involved in neuronal growth and function (Coffey et al., 2000; Waetzig and Herdegen, 2005). Interestingly, the removal of DLK does not appear to significantly affect the nonstress levels of p-JNK as judged by Western blotting and staining of neuronal cultures, and the alterations in p-JNK levels even after NGF withdrawal are relatively small compared with the changes observed in stress-specific JNK targets such as p-c-Jun (Fig. 2). The same is not true when neuronal MAPKKKs are broadly

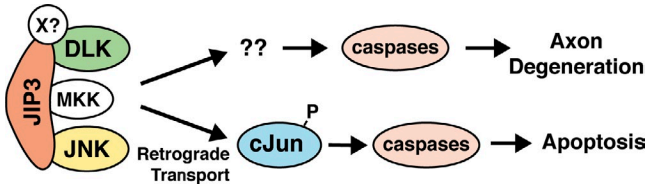

Figure 8. **A model for the regulation of developmental apoptosis and axon degeneration by DLK.** A complex containing DLK, JIP3, JNK, and possibly additional proteins (shown as protein X) is activated in the distal axon after NGF withdrawal and results in caspase-dependent neuronal apoptosis and axonal degeneration. Apoptosis occurs via retrograde transport of JNK and phosphorylation (P) of c-Jun, but axon degeneration does not require c-Jun and is mediated by distinct JNK targets.

inhibited by compounds such as CEP-1347, which results in a large reduction of total p-JNK levels (Maroney et al., 1998), suggesting that DLK is able to selectively modulate a subset of JNK activity, resulting in phosphorylation of specific targets without detectably altering the total levels of p-JNK within neurons.

How does DLK achieve such specific regulation of JNK activity? Our data demonstrate that DLK and JIP3 are components of a signaling complex, and knockdown of JIP3 displays an identical phenotype to loss of DLK in NGF-deprived neurons, implying that signaling specificity may be mediated by this interaction. It has been hypothesized that the binding of specific combinations of MAPKs to scaffolding proteins can generate diverse signaling complexes with distinct sets of downstream targets (Waetzig and Herdegen, 2005), though few examples of such complexes exist for which a specialized function has been identified. We propose that DLK–JIP3–JNK is an example of such a complex, which is able to selectively regulate stress-induced JNK activity in the context of NGF deprivation (Fig. 8). The observation that JIP1 does not provide similar neuronal protection provides additional rationale that this is a specific function of DLK bound to JIP3. Redistribution of p-JNK observed after NGF withdrawal likely also plays an important role in degeneration and may be required to position p-JNK proximal to substrates such as c-Jun. Indeed, nuclear localization of JNK has been shown to be required for neuronal apoptosis (Björkblom et al., 2008), and a similar relocalization has been observed in the context of axonal injury (Middlemas et al., 2003). We show that both DLK and JIP3 are required for p-JNK relocalization in response to NGF withdrawal, arguing that it too is dependent on the DLK–JIP3 signaling complex. This is consistent with previous results that demonstrated that JIP3 can mediate retrograde transport of JNK in response to axonal injury through interactions with the P150-glued subunit of the dynein motor protein complex (Cavalli et al., 2005), and it is conceivable that DLK–JNK interaction with JIP3 mediates retrograde transport of JNK after NGF withdrawal as well.

It is also possible that the signaling specificity downstream of DLK is mediated by activation of only a subset of the three JNK genes in mouse, all of which are expressed in embryonic neurons. The phenotypes observed in JNK-null mice argue that JNK2 and JNK3 are largely responsible for the JNK-mediated neuronal degeneration, at least in the context of injury (Bogoyevitch, 2006). Furthermore, JIP3 has been shown to preferentially interact with JNK3 over other JNK isoforms (Ito et al., 1999), raising the possibility that a significant amount of DLK–JIP3 signaling after NGF withdrawal could occur via JNK3. On the other hand, experiments in primary neurons have demonstrated that pan-JNK inhibition is sometimes required to provide complete rescue from degeneration (Björkblom et al., 2008), arguing that other JNK genes can also contribute to this process. Our data demonstrate that phosphorylation of both the 46- and 55-kD JNK bands is increased after NGF withdrawal and implies that multiple JNKs become activated, though it is possible that this pattern represents phosphorylation of different splice forms of a single JNK gene (Gupta et al., 1996). However, we also observed that knockout or siRNA-based knockdown of any individual JNK gene was not sufficient to provide protection after NGF withdrawal (unpublished data). This suggests that degeneration is likely mediated by a combination of JNK genes and that additional components of the pathway such as DLK and/or JIPs are necessary for regulation of prodegeneration-specific JNK activity.

c-Jun–independent functions of DLK–JNK in degeneration

The c-Jun–independent regulation of axon degeneration by DLK–JNK makes a strong case that phosphorylation of additional downstream targets is required for DLK-dependent neuronal degeneration. Several transcription factors can be phosphorylated by JNKs, including ATF2 (Widmann et al., 1999), and may contribute to the breakdown of axons. The DLK-dependent relocalization of p-JNK to the nucleus after NGF withdrawal agrees with this hypothesis. However, the observation that local axon degeneration is modulated by DLK–JNK suggests a possible alternative scenario in which this process is regulated via phosphorylation of axonal JNK targets. A local nontranscriptional role in axons would be consistent with the observation that both loss of DLK and pharmacological JNK inhibition protect from Wallerian degeneration after axotomy (Miller et al., 2009), in which the involvement of transcription is not possible. Several cytosolic JNK targets have been identified in neurons that may contribute to this degeneration, including doublecortin, SCG10, and Tau (Goedert et al., 1997; Gdalyahu et al., 2004; Tararuk et al., 2006). In addition, evidence exists in other systems that JNK is able to phosphorylate members of the intrinsic apoptotic machinery, including Bcl-2–associated death promoter and Bcl-2–like protein 11 (Donovan et al., 2002; Putcha et al., 2003). Phosphorylation of these substrates in axons may also contribute to degeneration, which is consistent with our finding that caspase activity in the axon can be modulated by DLK–JNK independent of c-Jun.

In summary, we have demonstrated that DLK is required for neuronal degeneration in peripherally projecting neuronal populations during development and is the primary MAPKKK upstream of c-Jun activation in this context. Although first described in developmental NGF withdrawal paradigms, the proapoptotic functions of c-Jun have since been shown to be conserved in neuronal injury and neurodegenerative disease. If DLK is required for JNK–c-Jun activation in the disease setting as well, targeting this kinase may represent an attractive approach for therapeutic intervention.

Materials and methods

Mouse models

DLK knockout mice were generated by homologous recombination using a phosphoglycerate kinase–neomycin cassette flanked by homology arms of 5.1 and 2.8 kb. The 5′ arm contained a LoxP site 1.5 kb away from the neomycin cassette. Embryonic stem (ES) cells were screened via PCR with the following primers, which amplified over both homology arms: 5′-AGGGGATAGTACAGCTCTGTGG-3′, 5′-CTGCGTGCAATCCATCTTG-3′ (5′ arm), 5′-CTTGTCGATCAGGATGATCTGG-3′, and 5′-CTACTGTCATCAAAGCTGCCAC-3′ (3 arm). The primers were confirmed via Southern blotting. Transfection of ES cells with a Cre-expressing plasmid resulted in recombination, which was assessed with the following primes: 5′-CACATCCTAGCCAAGTGCTCTAC-3′, 5′-ATCTGCCTTGTGTACCTGGGA-3′, and 5′-CTTGGGGACTAAGGTCAGTGAC-3′. HB9:GFP mice were obtained from S. Pfaff (Salk Institute, La Jolla, CA) and have been previously described (Lee et al., 2004). c-Jun knockout mice were obtained from E. Wagner (Centro Nacional de Investigaciones Oncológicas, Madrid, Spain), have been previously described (Behrens et al., 2002), and were crossed to Nestin-Cre (Jackson ImmunoResearch Laboratories, Inc.) to eliminate c-Jun expression in neurons.

Primary neuron culture

E13.5 DRGs were dissected and cultured in F12 media containing N3 supplement, glucose, and 25 ng/ml NGF on precoated poly-D-lysine and laminin chamber slides (BioCoat; BD). In DRG explant experiments 24 h after plating, media were replaced with media containing no NGF and 25 µg/ml anti-NGF antibody (Genentech) for various time periods and were then fixed for staining. For dissociated cultures, DRGs were digested in 0.05% trypsin for 30 min at 37°C and were plated as described above. 24 h after plating, mitotic inhibitor (cytosine arabinofuranoside [AraC]) was added to the culture and then removed 24 h later. NGF was withdrawn from the culture 4–5 d after plating as described above. In experiments using JNK inhibitor AS601245 (also known as JNK inhibitor V; EMD), 10 mM stock solution was made in DMSO and diluted to 10 µM working concentration in media. Compartmentalized chamber assays were performed essentially as previously described (Nikolaev et al., 2009). In brief, 35-mm tissue culture dishes were coated with poly-D-lysine and laminin and scratched with a pin rake (Tyler Research) to generate tracks for axonal growth. 50 ml of culture media containing 4 mg/ml methylcellulose was placed on the scratched area so that axons could grow within the tracks. A Teflon divider (Camp8; Tyler Research) that creates a central cell body chamber flanked by two axon chambers was then seated on silicone grease and placed on the culture dish as such that the cell body chamber was in the middle of the scratched area. Dissociated DRGs from E13.5 mouse embryos were suspended in methylcellulose-thickened medium and loaded in the cell body compartment, and both axon compartments were filled with culture media with 4 mg/ml methylcellulose. 1 d after plating, media containing 7 mM AraC were added to the cell body compartment for a period of 24 h. 3–5 d after plating, NGF was withdrawn from different compartments by replacing media containing 4 mg/ml methylcellulose and 25 mg/ml anti-NGF antibody.

For siRNA experiments, dissociated DRGs were transfected with siRNA using a nucleofection system (Lonza). DLK siRNA (sense 5′-GCACTGAATTGGACAACTCTT-3′ and antisense 5′-GAGTTGTCCAATTCAGTGCTT-3′) was synthesized at Genentech, and JIP1 (sc-35723; Santa Cruz Biotechnology, Inc.) and two siRNAs targeted to different regions of JIP3 (SI01300789 and SI01300796; QIAGEN) were purchased. Levels of knockdown were tested by quantitative PCR at 5 d after plating using the Syber green qPCR kit (QIAGEN) and verified primer sets (QIAGEN) for JIP1, JIP3, and DLK. The control siRNA used was an siRNA directed against luciferase. Glyceraldehyde 3-phosphate dehydrogenase expression level was used as a control for all samples. Quantitative PCR was analyzed by the Δ–ΔCT method comparing expression levels to the level of expression in control siRNA. Quantitative PCR was performed in triplicate ($n \geq 2$ experiments for each siRNA).

Immunocytochemistry and immunohistochemistry

Cultured neurons were fixed with 4% PFA and 15% sucrose for 30 min at room temperature, were blocked and permeabilized in PBS with 5% BSA and 0.2% Triton X-100 for 1 h, and were then stained overnight in blocking buffer, which contained the following antibodies: p-JNK, p-c-Jun serine 63 total JNK, ERK, p-ERK, cleaved caspase 3, cleaved caspase 9 (Cell Signaling Technology), Neuronal Class III β-tubulin (TuJ-1; Covance), NuN (Millipore), JIP3 (Novus Biologicals), JIP1 (Abcam), and DLK (generated using recombinant protein consisting of DLK A597-P888; provided by S. Hirai [Yokohama City University, Japan] or Genentech; Hirai et al., 2005). Slides were washed three times in PBS, incubated for 1 h at room temperature with Alexa Fluor–conjugated secondary antibodies (Invitrogen) followed by 3× PBS washes, and mounted in Fluoromount-G. Staining of tissue was performed using the protocol above but with PBS containing 5% normal goat serum and 0.1% Triton X-100 on 20-µm transverse sections cut on a cryostat. The antibodies used were pan-Trk (Cell Signaling Technology), activated caspase 3 (R&D Systems), HB9 (a gift from S. Pfaff), and Alexa Fluor–conjugated secondary antibodies (Invitrogen). For whole-mount embryo neurofilament staining, embryos were eviscerated, fixed in 4% PFA, and stained with rabbit anti-Neurofilament antibody (Covance) using the same protocol as described above, except that all antibody incubations were overnight, and buffers included 0.4% Triton X-100.

Western blotting and IP

DRG cultures were lysed in 100 µl Triton X-100 lysis buffer (20 mM Tris, pH 7.5, 150 mM NaCl, 0.1% Triton X-100, and protease and phosphatase inhibitors) for 30 min at 4°C. Because of the limited amount of protein harvested from DRGs, protein was precipitated using TCA and then washed with acetone three times to remove the residual TCA. The pellet was dried and resuspended in 1× SDS NuPAGE loading buffer containing a reducing agent. The amount of protein in samples was quantified by Western blotting for tubulin. Similar amounts of protein were then loaded on 4–12% Bis-Tris gels and subjected to standard immunoblotting procedures. Primary antibodies used for Western blotting were the same as those used for immunocytochemistry. Blot images were taken and quantified using the VersaDoc system (Bio-Rad Laboratories). p-JNK (upper band) and p-ERK (lower band) were quantified by normalizing to total levels of JNK and ERK, respectively, and were then compared with wt control or control siRNA with NGF. p-c-Jun quantification was also normalized to wt/control siRNA with NGF present. Each experiment for Western blots on $DLK^{-/-}$ neurons was performed with more than or equal to three embryos for each condition and repeated three times, whereas siRNA knockdown Western blots used electroporated DRG neurons from five embryos for each condition and were repeated more than or equal to two times. The p-JNK and p-c-Jun time course blots were performed with more than or equal to two embryos for each genotype at each time point.

IP studies in HEK-293 cells used a full-length mouse coding sequence of N-terminal Flag-tagged DLK, N-terminal Myc-tagged JIP3, and GFP expressed using Fugene6. 20 h after transfection, cells were washed with cold PBS and were lysed in 100 µl Triton X-100 lysis buffer (see above) for 30 min at 4°C. The amount of protein was quantified using bicinchoninic acid protein assay reagent (Thermo Fisher Scientific), and 200 µg of protein was taken for IP using a Flag IP kit (Sigma-Aldrich). 5% of protein was run as input, whereas 30% of the IP was run on Western blots. The IP experiment was repeated three times and showed similar results. For IP from mouse brain, whole brain was harvested from postnatal day 1 mice and lysed in buffer containing 1% Triton X-100, 150 mM NaCl, 50 mM Tris/HCl, and 1mM EDTA for 30 min at 4°C. IP was conducted using protein A–Sepharose beads and a DLK antibody (Genentech) or a rabbit IgG antibody. Beads were then washed twice in the lysis buffer followed by two washes in buffer without Triton X-100, and protein was then eluted in 1× SDS loading buffer containing a reducing agent. Equal amounts of brain lysate were added to each IP condition. Approximately 2% of the protein was run as input, whereas 30% of the pull-down was run in each lane of the Western blots and blotted with DLK (Genentech) or JIP3 (Novus Biologicals) antibody.

Imaging and quantification

Images of cultured neurons were acquired using a fluorescent microscope (DM5500; Leica) with a camera (DFC360) using a 20 or 40× objective, whereas whole-mount embryos and Trk-positive DRGs were imaged on a confocal microscope (LSM710; Carl Zeiss) using a 10 or 20× objective, respectively. Whole mounts were imaged as a flattened z stack and presented as maximum intensity projections. γ was altered to weak signal in compartmentalized chamber images shown in Fig. 5 and to more easily visualize neuritis in Figs. 6 (K and M) and S3 C using Photoshop (Adobe), but all data within a panel were identically imaged and modified. For all quantifications, values represent the mean of multiple experiments, and error bars represent SEM.

Axon degeneration in DRG explants and compartmentalized cultures was quantified blindly on a scale of 0–5, in which 0 equals no degeneration (equivalent to control cultures containing NGF) and 5 equals complete degeneration. Representative images were used to define intermediate stages of degeneration. For explant experiments, $n = 5$ embryos

with more than three explants scored per embryo. For compartmentalized chamber experiments, more than four chambers were quantified in two independent experiments. Axon degeneration quantification in dissociated DRG neurons was conducted using MetaMorph software (Molecular Devices). A journal that quantifies intact axons only was written and used to quantify all images, giving a total neurite length as a final readout for each image. Total neurite length in each condition was normalized to total neurite length in control wells containing NGF. More than or equal to three representative images from each experiment were quantified, and the data presented are representative of three independent experiments.

Quantifications of caspase 3 staining in dissociated DRG neurons were conducted manually by counting individual caspase 3/Tuj1-positive cell bodies. Three to five fields of each condition were quantified, and data are representative of at least two independent experiments. Caspase 9 staining in DRG axons was quantified using a relative scale of 0–5, in which 0 indicates that no axons are stained, and 5 indicates that all axons are stained. $n = 3$ embryos for each genotype with more than three explants scored per embryo.

p-c-Jun staining in compartmentalized chambers was quantified by blindly counting number of p-c-Jun–stained cells and normalizing to the number of DAPI-positive cells. Four regions from two independent experiments were quantified. p-JNK relocalization within neurons was quantified by measuring mean pixel intensity and total area of p-JNK that was either coincident or not coincident with neuronal nuclei (NeuN)–stained regions. Mean pixel intensity was then multiplied by area to generate a total pixel intensity for each region. The total pixel intensity associated with NeuN was then divided by the total pixel intensity of the image. Four regions from two independent experiments were quantified.

In vivo cell counts were quantified by counting the number of Trk-positive cells on each section and were normalized to DRG area on each section using ImageJ (National Institutes of Health). At least 8–10 sections were quantified per embryo, with $n = 3$ embryos per genotype. Quantification of activated caspase 3 was conducted using the same method ($n = 5$ embryos per genotype; a total of ≤25 DRG sections was quantified per genotype). For HB9 staining, numbers of positive neurons/motor column were manually counted in 8–10 lower lumbar sections per embryo, with $n = 3$ embryos quantified from each developmental stage and genotype. All counts were performed blind to genotype.

Online supplemental material

Fig. S1 shows the strategy used to generate DLK knockout mice. Fig. S2 shows that $DLK^{-/-}$ DRG neurons display normal growth. Fig. S3 shows the timing of JNK and c-Jun phosphorylation and p-JNK localization in wt and $DLK^{-/-}$ DRG neurons after NGF withdrawal. Fig. S4 shows that DLK, JIP1, and JIP3 siRNAs specifically knock down target gene expression. Fig. S5 shows that motor and sensory projections are normal in $DLK^{-/-}$ embryos at E12.5. Online supplemental material is available at http://www.jcb.org/cgi/content/full/jcb.201103153/DC1.

All authors on the study are employees of Genentech, Inc.. We thank Merone Roose Girma and the Genentech Transgenic facility for their assistance in generation of DLK knockout mice, Jeffrey Eastham-Anderson for helping with automated quantification, Syu-ichi Hirai for providing DLK antibodies, and Sam Pfaff for generously providing HB9 antibody and HB9:GFP mice. We also thank Marc Tessier-Lavigne, Morgan Sheng, Sarah Huntwork-Rodriguez, and others for helpful discussions and their critical review of the manuscript.

Submitted: 29 March 2011
Accepted: 3 August 2011

References

Arber, S., B. Han, M. Mendelsohn, M. Smith, T.M. Jessell, and S. Sockanathan. 1999. Requirement for the homeobox gene Hb9 in the consolidation of motor neuron identity. *Neuron*. 23:659–674. doi:10.1016/S0896-6273(01)80026-X

Behrens, A., M. Sibilia, J.P. David, U. Möhle-Steinlein, F. Tronche, G. Schütz, and E.F. Wagner. 2002. Impaired postnatal hepatocyte proliferation and liver regeneration in mice lacking c-jun in the liver. *EMBO J.* 21:1782–1790. doi:10.1093/emboj/21.7.1782

Besirli, C.G., E.F. Wagner, and E.M. Johnson Jr. 2005. The limited role of NH2-terminal c-Jun phosphorylation in neuronal apoptosis: identification of the nuclear pore complex as a potential target of the JNK pathway. *J. Cell Biol.* 170:401–411. doi:10.1083/jcb.200501138

Björkblom, B., N. Ostman, V. Hongisto, V. Komarovski, J.J. Filén, T.A. Nyman, T. Kallunki, M.J. Courtney, and E.T. Coffey. 2005. Constitutively active cytoplasmic c-Jun N-terminal kinase 1 is a dominant regulator of dendritic architecture: role of microtubule-associated protein 2 as an effector. *J. Neurosci.* 25:6350–6361. doi:10.1523/JNEUROSCI.1517-05.2005

Björkblom, B., J.C. Vainio, V. Hongisto, T. Herdegen, M.J. Courtney, and E.T. Coffey. 2008. All JNKs can kill, but nuclear localization is critical for neuronal death. *J. Biol. Chem.* 283:19704–19713. doi:10.1074/jbc.M707744200

Bogoyevitch, M.A. 2006. The isoform-specific functions of the c-Jun N-terminal Kinases (JNKs): differences revealed by gene targeting. *Bioessays*. 28:923–934. doi:10.1002/bies.20458

Brandon, E.P., W. Lin, K.A. D'Amour, D.P. Pizzo, B. Dominguez, Y. Sugiura, S. Thode, C.P. Ko, L.J. Thal, F.H. Gage, and K.F. Lee. 2003. Aberrant patterning of neuromuscular synapses in choline acetyltransferase-deficient mice. *J. Neurosci.* 23:539–549.

Campenot, R.B. 1977. Local control of neurite development by nerve growth factor. *Proc. Natl. Acad. Sci. USA*. 74:4516–4519. doi:10.1073/pnas.74.10.4516

Cavalli, V., P. Kujala, J. Klumperman, and L.S. Goldstein. 2005. Sunday Driver links axonal transport to damage signaling. *J. Cell Biol.* 168:775–787. doi:10.1083/jcb.200410136

Chang, L., Y. Jones, M.H. Ellisman, L.S. Goldstein, and M. Karin. 2003. JNK1 is required for maintenance of neuronal microtubules and controls phosphorylation of microtubule-associated proteins. *Dev. Cell*. 4:521–533. doi:10.1016/S1534-5807(03)00094-7

Coffey, E.T., V. Hongisto, M. Dickens, R.J. Davis, and M.J. Courtney. 2000. Dual roles for c-Jun N-terminal kinase in developmental and stress responses in cerebellar granule neurons. *J. Neurosci.* 20:7602–7613.

Collins, C.A., Y.P. Wairkar, S.L. Johnson, and A. DiAntonio. 2006. Highwire restrains synaptic growth by attenuating a MAP kinase signal. *Neuron*. 51:57–69. doi:10.1016/j.neuron.2006.05.026

Crowley, C., S.D. Spencer, M.C. Nishimura, K.S. Chen, S. Pitts-Meek, M.P. Armanini, L.H. Ling, S.B. McMahon, D.L. Shelton, A.D. Levinson, et al. 1994. Mice lacking nerve growth factor display perinatal loss of sensory and sympathetic neurons yet develop basal forebrain cholinergic neurons. *Cell*. 76:1001–1011. doi:10.1016/0092-8674(94)90378-6

Deckwerth, T.L., J.L. Elliott, C.M. Knudson, E.M. Johnson Jr., W.D. Snider, and S.J. Korsmeyer. 1996. BAX is required for neuronal death after trophic factor deprivation and during development. *Neuron*. 17:401–411. doi:10.1016/S0896-6273(00)80173-7

Donovan, N., E.B. Becker, Y. Konishi, and A. Bonni. 2002. JNK phosphorylation and activation of BAD couples the stress-activated signaling pathway to the cell death machinery. *J. Biol. Chem.* 277:40944–40949. doi:10.1074/jbc.M206113200

Garcia, I., I. Martinou, Y. Tsujimoto, and J.C. Martinou. 1992. Prevention of programmed cell death of sympathetic neurons by the bcl-2 proto-oncogene. *Science*. 258:302–304. doi:10.1126/science.1411528

Gdalyahu, A., I. Ghosh, T. Levy, T. Sapir, S. Sapoznik, Y. Fishler, D. Azoulai, and O. Reiner. 2004. DCX, a new mediator of the JNK pathway. *EMBO J.* 23:823–832. doi:10.1038/sj.emboj.7600079

Goedert, M., M. Hasegawa, R. Jakes, S. Lawler, A. Cuenda, and P. Cohen. 1997. Phosphorylation of microtubule-associated protein tau by stress-activated protein kinases. *FEBS Lett.* 409:57–62. doi:10.1016/S0014-5793(97)00483-3

Gorin, P.D., and E.M. Johnson. 1979. Experimental autoimmune model of nerve growth factor deprivation: effects on developing peripheral sympathetic and sensory neurons. *Proc. Natl. Acad. Sci. USA*. 76:5382–5386. doi:10.1073/pnas.76.10.5382

Gupta, S., T. Barrett, A.J. Whitmarsh, J. Cavanagh, H.K. Sluss, B. Dérijard, and R.J. Davis. 1996. Selective interaction of JNK protein kinase isoforms with transcription factors. *EMBO J.* 15:2760–2770.

Ham, J., C. Babij, J. Whitfield, C.M. Pfarr, D. Lallemand, M. Yaniv, and L.L. Rubin. 1995. A c-Jun dominant negative mutant protects sympathetic neurons against programmed cell death. *Neuron*. 14:927–939. doi:10.1016/0896-6273(95)90331-3

Hammarlund, M., P. Nix, L. Hauth, E.M. Jorgensen, and M. Bastiani. 2009. Axon regeneration requires a conserved MAP kinase pathway. *Science*. 323:802–806. doi:10.1126/science.1165527

Hirai, S., A. Kawaguchi, J. Suenaga, M. Ono, D.F. Cui, and S. Ohno. 2005. Expression of MUK/DLK/ZPK, an activator of the JNK pathway, in the nervous systems of the developing mouse embryo. *Gene Expr. Patterns*. 5:517–523. doi:10.1016/j.modgep.2004.12.002

Hirai, S., F. Cui, T. Miyata, M. Ogawa, H. Kiyonari, Y. Suda, S. Aizawa, Y. Banba, and S. Ohno. 2006. The c-Jun N-terminal kinase activator dual leucine zipper kinase regulates axon growth and neuronal migration in the developing cerebral cortex. *J. Neurosci.* 26:11992–12002. doi:10.1523/JNEUROSCI.2272-06.2006

Hunot, S., M. Vila, P. Teismann, R.J. Davis, E.C. Hirsch, S. Przedborski, P. Rakic, and R.A. Flavell. 2004. JNK-mediated induction of cyclooxygenase 2 is

required for neurodegeneration in a mouse model of Parkinson's disease. *Proc. Natl. Acad. Sci. USA*. 101:665–670. doi:10.1073/pnas.0307453101

Ito, M., K. Yoshioka, M. Akechi, S. Yamashita, N. Takamatsu, K. Sugiyama, M. Hibi, Y. Nakabeppu, T. Shiba, and K.I. Yamamoto. 1999. JSAP1, a novel jun N-terminal protein kinase (JNK)-binding protein that functions as a Scaffold factor in the JNK signaling pathway. *Mol. Cell. Biol.* 19:7539–7548.

Itoh, A., M. Horiuchi, K. Wakayama, J. Xu, P. Bannerman, D. Pleasure, and T. Itoh. 2011. ZPK/DLK, a mitogen-activated protein kinase kinase kinase, is a critical mediator of programmed cell death of motoneurons. *J. Neurosci.* 31:7223–7228. doi:10.1523/JNEUROSCI.5947-10.2011

Lee, S.K., L.W. Jurata, J. Funahashi, E.C. Ruiz, and S.L. Pfaff. 2004. Analysis of embryonic motoneuron gene regulation: derepression of general activators function in concert with enhancer factors. *Development*. 131:3295–3306. doi:10.1242/dev.01179

Levi-Montalcini, R., and B. Booker. 1960. Destruction of the sympathetic ganglia in mammals by an antiserum to a nerve-growth protein. *Proc. Natl. Acad. Sci. USA*. 46:384–391. doi:10.1073/pnas.46.3.384

Lewcock, J.W., N. Genoud, K. Lettieri, and S.L. Pfaff. 2007. The ubiquitin ligase Phr1 regulates axon outgrowth through modulation of microtubule dynamics. *Neuron*. 56:604–620. doi:10.1016/j.neuron.2007.09.009

Luo, L., and D.D. O'Leary. 2005. Axon retraction and degeneration in development and disease. *Annu. Rev. Neurosci.* 28:127–156. doi:10.1146/annurev.neuro.28.061604.135632

Mack, T.G., M. Reiner, B. Beirowski, W. Mi, M. Emanuelli, D. Wagner, D. Thomson, T. Gillingwater, F. Court, L. Conforti, et al. 2001. Wallerian degeneration of injured axons and synapses is delayed by a Ube4b/Nmnat chimeric gene. *Nat. Neurosci.* 4:1199–1206. doi:10.1038/nn770

Maroney, A.C., M.A. Glicksman, A.N. Basma, K.M. Walton, E. Knight Jr., C.A. Murphy, B.A. Bartlett, J.P. Finn, T. Angeles, Y. Matsuda, et al. 1998. Motoneuron apoptosis is blocked by CEP-1347 (KT 7515), a novel inhibitor of the JNK signaling pathway. *J. Neurosci.* 18:104–111.

Middlemas, A., J.D. Delcroix, N.M. Sayers, D.R. Tomlinson, and P. Fernyhough. 2003. Enhanced activation of axonally transported stress-activated protein kinases in peripheral nerve in diabetic neuropathy is prevented by neurotrophin-3. *Brain*. 126:1671–1682. doi:10.1093/brain/awg150

Miller, B.R., C. Press, R.W. Daniels, Y. Sasaki, J. Milbrandt, and A. DiAntonio. 2009. A dual leucine kinase-dependent axon self-destruction program promotes Wallerian degeneration. *Nat. Neurosci.* 12:387–389. doi:10.1038/nn.2290

Mok, S.A., K. Lund, and R.B. Campenot. 2009. A retrograde apoptotic signal originating in NGF-deprived distal axons of rat sympathetic neurons in compartmented cultures. *Cell Res.* 19:546–560. doi:10.1038/cr.2009.11

Nakata, K., B. Abrams, B. Grill, A. Goncharov, X. Huang, A.D. Chisholm, and Y. Jin. 2005. Regulation of a DLK-1 and p38 MAP kinase pathway by the ubiquitin ligase RPM-1 is required for presynaptic development. *Cell*. 120:407–420. doi:10.1016/j.cell.2004.12.017

Nikolaev, A., T. McLaughlin, D.D. O'Leary, and M. Tessier-Lavigne. 2009. APP binds DR6 to trigger axon pruning and neuron death via distinct caspases. *Nature*. 457:981–989. doi:10.1038/nature07767

Oppenheim, R.W. 1991. Cell death during development of the nervous system. *Annu. Rev. Neurosci.* 14:453–501. doi:10.1146/annurev.ne.14.030191.002321

Palmada, M., S. Kanwal, N.J. Rutkoski, C. Gustafson-Brown, R.S. Johnson, R. Wisdom, and B.D. Carter. 2002. c-jun is essential for sympathetic neuronal death induced by NGF withdrawal but not by p75 activation. *J. Cell Biol.* 158:453–461. doi:10.1083/jcb.200112129

Putcha, G.V., S. Le, S. Frank, C.G. Besirli, K. Clark, B. Chu, S. Alix, R.J. Youle, A. LaMarche, A.C. Maroney, and E.M. Johnson Jr. 2003. JNK-mediated BIM phosphorylation potentiates BAX-dependent apoptosis. *Neuron*. 38:899–914. doi:10.1016/S0896-6273(03)00355-6

Schoenmann, Z., E. Assa-Kunik, S. Tiomny, A. Minis, L. Haklai-Topper, E. Arama, and A. Yaron. 2010. Axonal degeneration is regulated by the apoptotic machinery or a NAD+-sensitive pathway in insects and mammals. *J. Neurosci.* 30:6375–6386. doi:10.1523/JNEUROSCI.0922-10.2010

Tararuk, T., N. Ostman, W. Li, B. Björkblom, A. Padzik, J. Zdrojewska, V. Hongisto, T. Herdegen, W. Konopka, M.J. Courtney, and E.T. Coffey. 2006. JNK1 phosphorylation of SCG10 determines microtubule dynamics and axodendritic length. *J. Cell Biol.* 173:265–277. doi:10.1083/jcb.200511055

Vohra, B.P., Y. Sasaki, B.R. Miller, J. Chang, A. DiAntonio, and J. Milbrandt. 2010. Amyloid precursor protein cleavage-dependent and -independent axonal degeneration programs share a common nicotinamide mononucleotide adenylyltransferase 1-sensitive pathway. *J. Neurosci.* 30:13729–13738. doi:10.1523/JNEUROSCI.2939-10.2010

Waetzig, V., and T. Herdegen. 2005. Context-specific inhibition of JNKs: overcoming the dilemma of protection and damage. *Trends Pharmacol. Sci.* 26:455–461.

Watts, R.J., E.D. Hoopfer, and L. Luo. 2003. Axon pruning during *Drosophila* metamorphosis: evidence for local degeneration and requirement of the ubiquitin-proteasome system. *Neuron*. 38:871–885. doi:10.1016/S0896-6273(03)00295-2

White, F.A., I. Silos-Santiago, D.C. Molliver, M. Nishimura, H. Phillips, M. Barbacid, and W.D. Snider. 1996. Synchronous onset of NGF and TrkA survival dependence in developing dorsal root ganglia. *J. Neurosci.* 16:4662–4672.

White, F.A., C.R. Keller-Peck, C.M. Knudson, S.J. Korsmeyer, and W.D. Snider. 1998. Widespread elimination of naturally occurring neuronal death in Bax-deficient mice. *J. Neurosci.* 18:1428–1439.

Whitfield, J., S.J. Neame, L. Paquet, O. Bernard, and J. Ham. 2001. Dominant-negative c-Jun promotes neuronal survival by reducing BIM expression and inhibiting mitochondrial cytochrome c release. *Neuron*. 29:629–643. doi:10.1016/S0896-6273(01)00239-2

Whitmarsh, A.J. 2006. The JIP family of MAPK scaffold proteins. *Biochem. Soc. Trans.* 34:828–832. doi:10.1042/BST0340828

Widmann, C., S. Gibson, M.B. Jarpe, and G.L. Johnson. 1999. Mitogen-activated protein kinase: conservation of a three-kinase module from yeast to human. *Physiol. Rev.* 79:143–180.

Xiong, X., X. Wang, R. Ewanek, P. Bhat, A. Diantonio, and C.A. Collins. 2010. Protein turnover of the Wallenda/DLK kinase regulates a retrograde response to axonal injury. *J. Cell Biol.* 191:211–223. doi:10.1083/jcb.201006039

Xu, Z., A.C. Maroney, P. Dobrzanski, N.V. Kukekov, and L.A. Greene. 2001. The MLK family mediates c-Jun N-terminal kinase activation in neuronal apoptosis. *Mol. Cell. Biol.* 21:4713–4724. doi:10.1128/MCB.21.14.4713-4724.2001

Yang, D.D., C.Y. Kuan, A.J. Whitmarsh, M. Rincón, T.S. Zheng, R.J. Davis, P. Rakic, and R.A. Flavell. 1997. Absence of excitotoxicity-induced apoptosis in the hippocampus of mice lacking the Jnk3 gene. *Nature*. 389:865–870. doi:10.1038/39899